

Monte Carlo Turbulence Simulation Using Rational Approximations to von Kármán Spectra

C. Warren Campbell*

NASA Marshall Space Flight Center, Alabama

Turbulence simulation is computationally much simpler using rational spectra, but turbulence falls off as $f^{-5/3}$ in frequency ranges of interest to aircraft response and as predicted by von Kármán's model. Rational approximations to von Kármán spectra should satisfy three requirements: 1) The rational spectra should provide a good approximation to the von Kármán spectra in the frequency range of interest; 2) for stability, the resulting rational transfer function should have all its poles in the left half-plane; and 3) at high frequencies, the rational spectra must fall off as an integer power of frequency, and since the -2 power is closest to the $-5/3$ power, the rational approximation should roll off as the -2 power at high frequencies. Rational approximations to von Kármán spectra that satisfy these three criteria are presented, along with spectra from simulated turbulence. Agreement between the spectra of the simulated turbulence and von Kármán spectra is excellent.

Nomenclature

a	= von Kármán constant, = 1.339
A, B, C, D, F	= coefficients corresponding to different poles of the rational spectra
$E_{ij(ij)}$	= a convenient exponential notation, = $\exp(p_i T) + \exp(p_j T) + \exp((p_i + p_j)T)$ = $E_i + E_j + E_{(ij)}$
f	= frequency, Hz
f_s	= sampling frequency, Hz
H_L, H_T	= longitudinal and transverse transfer functions, respectively
k_l	= coefficient of the longitudinal approximation spectra
k_T	= coefficient of the transverse approximation spectra
l_i	= coefficient of y_{n-1} in the turbulence generation difference equation
L	= length scale of turbulence as appropriate for the spectrum under consideration, i.e., either longitudinal or transverse
p_i	= i th pole of the approximation spectrum
p_i'	= i th dimensionless pole of approximation spectrum = p_i/α
r_i	= coefficient of x_{n-1} in the turbulence generation difference equation
s	= Laplace transforms
t	= time
T	= sampling interval
V	= airspeed of aircraft
$x(t)$	= wide-band Gaussian noise
$X(s)$	= Laplace transform of input noise $x(t)$
$y(t)$	= output simulated turbulence
$Y(s)$	= Laplace transform of output turbulence $y(t)$
z_i	= i th zero of approximation spectrum
α	= VT/L
σ	= rms turbulent velocity
$\hat{\sigma}$	= discrete turbulence rms value
ϕ_L	= longitudinal spectrum
ϕ_T	= transverse spectrum

Introduction

THE purpose of Monte Carlo turbulence simulation is to generate time histories that have the statistical character of atmospheric turbulence. The simulated turbulence is then used to create an atmospheric simuland for the purpose of flight simulation. Several techniques may be used for implementing the turbulence simulation, but rational turbulence spectra permit the generation of difference equations with a tremendous computational advantage over methods corresponding to irrational spectra. Real atmospheric spectra tend to roll off as $f^{-5/3}$, however.

Some earlier efforts to approximate von Kármán spectra were made. Wang and Frost¹ show an approximation spectrum that does not fit the von Kármán spectrum very well. Tatom and Smith² attempted to fit the von Kármán spectrum with a rational function. While the spectrum was an accurate fit, the resulting difference equations were unstable. This paper documents a technique that satisfies the following three criteria for rational approximations to the realistic von Kármán spectrum.

1) The spectra are good approximations to the von Kármán model within the frequency ranges of interest for aircraft response.

2) The transfer functions corresponding to the approximation spectra represent stable systems, i.e., all poles are in the left half plane.

3) At high frequencies the approximation spectra fall off as f^{-2} .

The reasons for the computational advantages of techniques corresponding to rational spectra are discussed in some detail. Approximation spectra based on a continued fraction expansion of the binomial function are presented with corresponding difference equations. Comparisons of generated turbulent spectra with von Kármán theoretical spectra are presented.

Rational vs Irrational Generation Techniques

Monte Carlo turbulence is commonly generated as shown in Fig. 1. A wide-band, white noise source is input to a filter. The transfer function of the filter is chosen so that the output spectrum matches the desired turbulence spectrum. If the input noise is Gaussian and the filter linear, the output will also be Gaussian.

The best known turbulence spectral models are the rational Dryden model and the irrational, but more realistic, von Kármán model. The Dryden spectral model may be regarded as a rational approximation to the von Kármán model. Unfor-

Received Oct. 31, 1984; revision received March 25, 1985. This paper is a work of the U.S. Government and therefore is in the public domain.

*Aerospace Engineer, Systems Dynamics Laboratory. Member AIAA.

unately, the Dryden model is not a very good approximation to the von Kármán model over frequency ranges of interest for atmospheric turbulence simulation.

Rational spectra are desirable because generation techniques are computationally more efficient than those for irrational spectra. The Dryden model transfer function corresponding to the longitudinal velocity is given by

$$H_L(s) = a_1/(s + b_1) \quad (1)$$

$H_L(s) = Y(s)/X(s)$ can be substituted in Eq. (1) and rearranged into the following convenient form:

$$(s + b_1)Y(s) = a_1X(s) \quad (2)$$

The inverse Laplace transform of Eq. (2) yields the following ordinary differential equation with constant coefficients:

$$\frac{dy}{dt} + b_1y = a_1x \quad (3)$$

This simple equation can be discretized to yield a simple explicit difference equation for the efficient generation of simulated turbulence.

Similarly for the von Kármán model, the irrational transfer function is given by

$$H_L(s) = c_1/(d_1 + s)^{5/6} \quad (4)$$

The corresponding equation to Eq. (2) is

$$(d_1 + s)^{5/6}Y(s) = c_1X(s) \quad (5)$$

Previously, Y was multiplied by s , which corresponds to taking a derivative in the time domain. In the irrational case, we have terms like $s^{5/6}$. Heuristically $(d_1 + s)^{5/6}$ can be expanded in an infinite series to yield the following result.

$$\begin{aligned} (d_1 + s)^{5/6} &= d_1^{5/6} + 5/6d_1^{-1/6}s - 5/72d_1^{-7/6}s^2 \\ &+ 35/1296d_1^{-13/6}s^3 - \dots \end{aligned} \quad (6)$$

The corresponding differential equation is

$$\begin{aligned} y(t)d_1^{5/6} + 5/6d_1^{-1/6}\frac{dy}{dt} - 5/72d_1^{-7/6}\frac{d^2y}{dt^2} \\ + 35/1296d_1^{-13/6}\frac{d^3y}{dt^3} - \dots = c_1x \end{aligned} \quad (7)$$

In the irrational case, the differential equation is given by a linear ordinary differential equation with constant coefficients as before, but of infinite order. Obviously Eq. (7) cannot be discretized to obtain a simple difference equation. Instead the noise must be generated in a block, transformed to the frequency domain with a fast Fourier transform (FFT), multiplied point by point by the desired filter function, and then transformed back to the time domain. This procedure is computationally much more complex and time consuming than simple difference equation techniques.

Table 1 summarizes the spectra, transfer functions, and differential equations for the von Kármán and Dryden turbulence models for each velocity component. From the table, the lateral and vertical functions have the same form; thus,



Fig. 1 Monte Carlo turbulence simulation technique.

they are referred to herein as transverse functions. The constants shown in the table, e.g., a_1 or b_1 , are functions of L , V , etc. The constants for the Dryden model are not necessarily the same as those for the von Kármán functions. The form of the transfer functions was drawn from Ref. 1.

A rational approximation spectrum is described by Wang and Frost¹ that fails to satisfy criterion above. In the following section an approximation spectrum is derived that satisfies all three of the above criteria.

Derivation of Approximation Spectra

In the preceding section, an infinite series expansion of $(d_1 + s)^{5/6}$ was used to obtain an infinite order differential equation corresponding to the von Kármán model. The resulting differential equation cannot be discretized, but one wonders if it might not be truncated at some point to obtain a rational approximation. The equation was derived heuristically, and the infinite series does not even converge beyond the first singularity of the complex transfer function. The rational

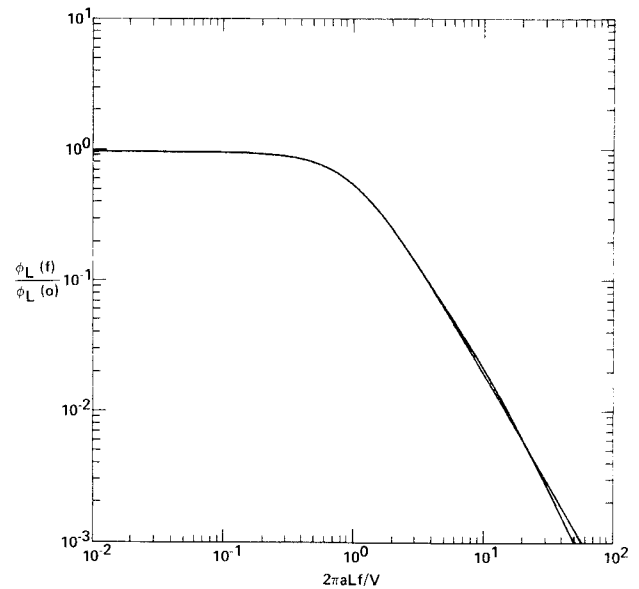


Fig. 2 Comparison of longitudinal normalized spectra for the von Kármán and rational models.

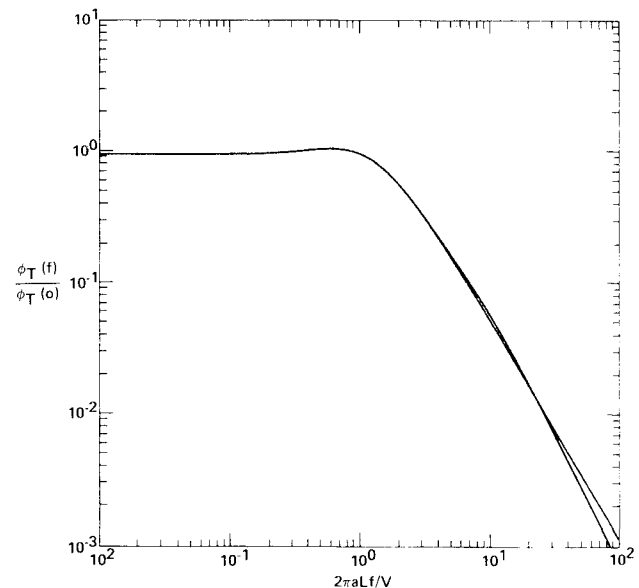


Fig. 3 Comparison of transverse normalized spectra for the von Kármán and rational models.

Table 1 Summary of transfer functions and spectra for Dryden and von Kármán models; one-dimensional models

	Longitudinal	Lateral	Vertical
	Dryden		
Spectra	$\phi_1 = \frac{\sigma_1^2 2L_1}{\pi} \frac{1}{1 + (2\pi L_1 f/V)^2}$	$\phi_2 = \frac{\sigma_2^2 L_2}{\pi} \frac{1 + 3(2\pi L_2 f/V)^2}{[1 + (2\pi L_2 f/V)^2]^2}$	$\phi_3 = \frac{\sigma_3^2 L_3}{\pi} \frac{1 + 3(2\pi L_3 f/V)^2}{[1 + (2\pi L_3 f/V)^2]^2}$
Transfer functions	$H_1(s) = \frac{C_1}{a_1 + s}$	$H_2(s) = \frac{C_2(b_2 + s)}{(a_2 + s)^2}$	$H_3(s) = \frac{C_3(b_3 + s)}{(a_3 + s)^2}$
ODE ^a	$\frac{dy}{dt} + a_1 y = C_1 X$	$\frac{d^2 y}{dt^2} + 2a_2 \frac{dy}{dt} + a_2^2 y = C_2 \left(\frac{dx}{dt} + b_2 x \right)$	$\frac{d^2 y}{dt^2} + 2a_3 \frac{dy}{dt} + a_3^2 y = C_3 \left(\frac{dx}{dt} + b_3 x \right)$
	von Kármán		
Spectra	$\phi_1 = \frac{\sigma_1^2 2L_1}{\pi} \frac{1}{[1 + (2\pi a L_1 f/V)^2]^{5/6}}$	$\phi_2 = \frac{\sigma_2^2 L_2}{\pi} \frac{1 + 8/3(2\pi a L_2 f/V)^2}{[1 + (2\pi a L_2 f/V)^2]^{11/6}}$	$\phi_3 = \frac{\sigma_3^2 L_3}{\pi} \frac{1 + 8/3(2\pi a L_3 f/V)^2}{[1 + (2\pi a L_3 f/V)^2]^{11/6}}$
Transfer functions	$H_1(s) = \frac{C_1}{(a_1 + s)^{5/6}}$	$H_2(s) = \frac{b_2(s + C_2)}{(s + a_2)^{11/6}}$	$H_3(s) = \frac{b_3(s + C_3)}{(s + a_3)^{11/6}}$
ODE ^a	Linear, infinite order ODE	Linear, infinite order ODE	Linear, infinite order ODE

^aOrdinary differential equation.

Padé approximant to the transfer function can be derived from the infinite series and may converge everywhere in the complex plane except at points of singularities. For a further discussion of this remarkable property of rational approximations see Van Dyke.³ The rational approximation spectra presented here are based on the well-known continued fraction expansion of the binomial function (see, e.g., Khovanskii⁴).

$$(1+s)^\nu = \frac{1}{1 - \frac{\nu s}{1 + \frac{(1+\nu)s}{2 + \frac{(1-\nu)s}{3 + \frac{(2+\nu)s}{2 + \frac{(2-\nu)s}{5 + \dots \frac{(n+\nu)s}{2 + \frac{(n-\nu)s}{(2n+1) + \dots}}}}}}}} \quad (8)$$

The infinite continued fraction of Eq. (8) converges throughout the infinite s plane except along the branch cut from $s = -1$ to $-\infty$. The fact that the continued fraction converges along the imaginary axis is important in what is to follow, because only the imaginary values of the transfer function affect the form of the spectrum. When truncated at the proper point it can provide the basis for a turbulence generation technique satisfying the three previously mentioned criteria. Doing the truncation, letting $\nu = -5/6$, and converting to the more conventional rational form yields the following approximation:

$$(1+s)^{-5/6} \approx \frac{60 + 52s + 91/12s^2}{60 + 102s + 561/12s^2 + 935/216s^3} \quad (9)$$

Poles and zeroes of the above approximation are presented in Table 2. Note that all of the poles fall in the left half-plane so that the corresponding differential system will be unconditionally stable. In fact, the poles all lie on the negative real axis, as do the zeroes. This means that the modulus of the transfer function evaluated on the imaginary axis is symmetric with respect to the origin. In general, all transfer function poles should lie on the negative real axis. Nothing is gained as

Table 2 Poles and zeroes of the approximation function

$p'_1 = -1.02025059$	$z'_1 = -1.468210716$
$p'_2 = -1.67661571$	$z'_2 = -5.388932143$
$p'_3 = -8.10313370$	

For transverse spectra, p'_1, p'_2, z'_1 , and z'_2 are as above. In addition:
 $p'_4 = -1$; $z'_3 = -(3/8)^{1/2}$

far as the spectrum is concerned by using complex poles since, for real spectra, the poles must occur in complex conjugate pairs. This is a direct result of the fact that a spectrum is a Fourier transform of an autocorrelation, which is a real and even function. The spectrum must also be real, even, and always positive.

The resulting transfer function may be multiplied by its complex conjugate to obtain the corresponding spectrum. Figure 2 shows the very favorable comparison between the approximation longitudinal spectrum and the von Kármán spectrum.

The transverse transfer function is slightly more complex, but can be developed from the same basic function as above by multiplying the numerator by the factor $(1 + (8/3)^{1/2}s)$ and the denominator by $(1+s)$. By so doing the transverse form is obtained. Observe that an additional pole is obtained at $s = -1$, along with a new zero. The new pole is in the left half-plane and the resulting system remains stable. Figure 3 presents the transverse approximation spectrum as compared to the corresponding von Kármán spectrum; again the comparison is very favorable.

The derived transfer functions are good approximations to the von Kármán spectra, represent stable continuous (analog) systems, and fall off as f^{-2} at high frequencies. The preceding criteria are therefore satisfied. The remaining task is to convert the continuous systems to stable, discrete systems, and this problem is treated in the following section.

Discretization of the Approximation Equations

The equations derived previously correspond to a pair of ordinary differential equations with constant coefficients. The problem is to discretize them in such a way that no matter

Table 3 Coefficients of the longitudinal equation

$$p_i = p'_i \alpha, \alpha = VT/L, k_1 = -\sigma(L/V\pi)^{1/2} (p_1 p_2 p_3)/(z_1 z_2) \\ \hat{\sigma} = 0.8672\alpha^{0.49626}$$

$$A = k_1(p_1 - z_1)(p_1 - z_2)/p_1(p_1 - p_2)(p_1 - p_3)$$

$$B = k_1(p_2 - z_1)(p_2 - z_2)/p_2(p_2 - p_1)(p_2 - p_3)$$

$$C = k_1(p_3 - z_1)(p_3 - z_2)/p_3(p_3 - p_1)(p_3 - p_2)$$

$$D = -k_1 z_1 z_2 / p_1 p_2 p_3$$

$$r_0 = A + B + C + D$$

$$r_1 = A(1 + E_{23}) + B(1 + E_{13}) + C(1 + E_{12}) + DE_{123}$$

$$r_2 = AE_{23(23)} + BE_{13(13)} + CE_{12(12)} + DE_{(12)(13)(23)}$$

$$r_3 = AE_{(23)} + BE_{(13)} + CE_{(12)} + DE_{(123)}$$

$$l_1 = E_{123}, l_2 = E_{(12)(13)(23)}, l_3 = E_{(123)}$$

what the sampling frequency, the systems remain stable. An approach that assures this is described by Neuman and Foster.⁵ When the approach is followed for the longitudinal velocity component, the resulting difference equation takes the following form:

$$y_n - l_1 y_{n-1} - l_2 y_{n-2} + l_3 y_{n-3} + r_0 x_n - r_1 x_{n-1} + r_2 x_{n-2} - r_3 x_{n-3} \quad (10)$$

The coefficients of this equation are presented in Table 3. Notice that the above equation is in explicit form, i.e., the current turbulence value depends only upon preceding values of turbulence and noise and *not* on any future turbulence value.

From Table 3 and Eq. (10), and the preceding discussion, one might expect that since the coefficients are functions of $\alpha = VT/L$, the variance of the resulting simulated turbulence would also be a function of α . This turns out to be the case, as was shown by Wang and Frost.¹ In the simple Dryden case, values of the variance as a function of α can be derived. In the case of the higher level approximation presented here, the derivation is much more difficult, and in fact was not done. Instead, 100,000 points of turbulence were generated at various values of α and rms values calculated. The resulting variation was quite smooth, and curves were fitted to the values. The equation for the variation of $\hat{\sigma}$ as a function of α is also included in Table 3.

In Table 3 a convenient notation is used. The best way to explain the shorthand is to give a few simple examples. $E_{123} = \exp(p_1 T) + \exp(p_2 T) + \exp(p_3 T) = E_1 + E_2 + E_3$. $E_{(123)} = \exp(p_1 T + p_2 T + p_3 T)$. Terms inside parentheses go inside exponential parentheses as indicated in the second example. Finally, $E_{(12)(13)(23)} = E_{(12)} + E_{(13)} + E_{(23)} = \exp(p_1 T + p_2 T) + \exp(p_1 T + p_3 T) + \exp(p_2 T + p_3 T)$.

A similar approach can be taken for the transverse approximation spectrum. The resulting difference equation is

$$y_n = l_1 y_{n-1} - l_2 y_{n-2} + l_3 y_{n-3} - l_4 y_{n-4} + r_0 x_n \\ - r_1 x_{n-1} + r_2 x_{n-2} - r_3 x_{n-3} + r_4 x_{n-4} \quad (11)$$

The coefficients for the transverse case are presented in Table 4. Utilizing Tables 2-4, turbulence can be generated for each velocity component. Using a sampling frequency $f_s = 5$ Hz, length scale $L = 500$ m, and velocity $V = 100$ m/s, blocks of turbulence were generated and spectra calculated. Figures 4 and 5 present comparisons between the spectra of the simulated turbulence and corresponding von Kármán spectra. The agreement is excellent, and statistical scatter in the calculated spectra is much greater than the difference between approximation and von Kármán spectra. One caution should be mentioned concerning the use of the difference equations. The difference equations were derived using the z transform,

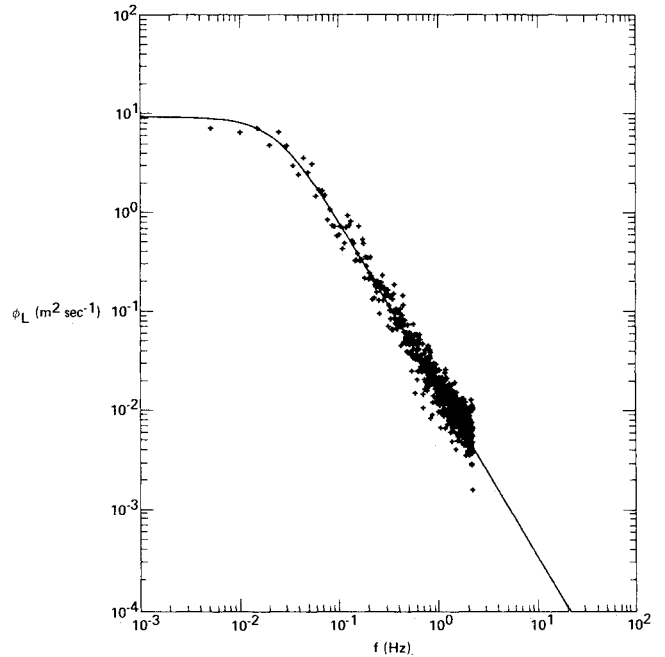


Fig. 4 Comparison of longitudinal simulation spectrum with von Kármán spectrum ($f_s = 5$ Hz, $V = 100$ m/s, $\sigma = 1.0$ m/s, $L = 500$ m).

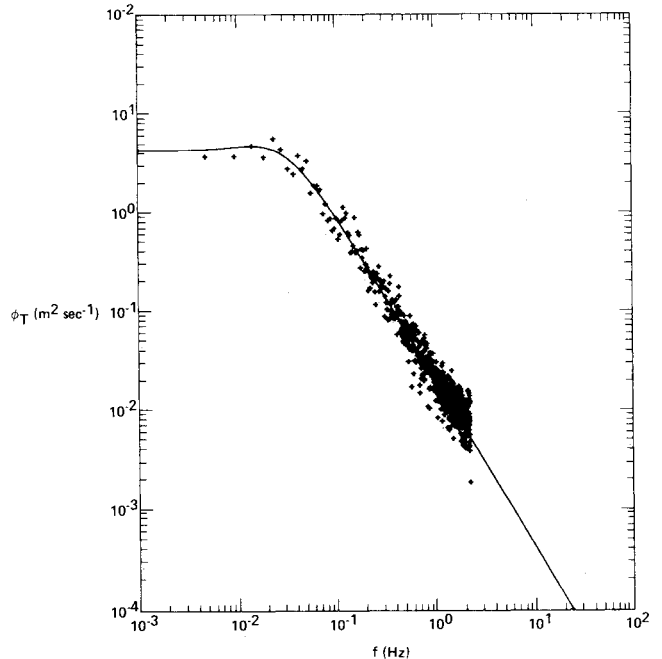


Fig. 5 Comparison of transverse simulation spectrum with von Kármán spectrum ($f_s = 5$ Hz, $V = 100$ m/s, $\sigma = 1.0$ m/s, $L = 500$ m).

which is the digital equivalent of the Laplace transform. The Laplace transform and the z transform incorporate initial values directly into the transform. The difference equations presented here were derived assuming zero initial conditions, and if zero initial conditions are not input to any coded version of the above equations, a large transient will result.

An algorithm for generating turbulence is given as follows.

- 1) Initialize the x_n and y_n to zero.
- 2) Obtain the current values of σ , L , and V .
- 3) Calculate all of the coefficients in Table 3 or 4 as appropriate.
- 4) Generate a new value of y using Eq. (10) or (11) as appropriate.

Table 4 Coefficients of the transverse equation

$$\hat{\sigma} = 1.233\alpha^{0.4976} \quad k_T = -\sigma(L/V\pi)^{1/2} (p_1 p_2 p_3 p_4) / (z_1 z_2 z_3)$$

$$A = k_T (p_1 - z_1)(p_1 - z_2)(p_1 - z_3) / p_1 (p_1 - p_2)(p_1 - p_3)(p_1 - p_4)$$

$$B = k_T (p_2 - z_1)(p_2 - z_2)(p_2 - z_3) / p_2 (p_2 - p_1)(p_2 - p_3)(p_2 - p_4)$$

$$C = k_T (p_3 - z_1)(p_3 - z_2)(p_3 - z_3) / p_3 (p_3 - p_1)(p_3 - p_2)(p_3 - p_4)$$

$$D = k_T (p_4 - z_1)(p_4 - z_2)(p_4 - z_3) / p_4 (p_4 - p_1)(p_4 - p_2)(p_4 - p_3)$$

$$F = -k_T z_1 z_2 z_3 / p_1 p_2 p_3 p_4$$

$$r_0 = A + B + C + D + F$$

$$r_1 = A(1 + E_{234}) + B(1 + E_{134}) + C(1 + E_{124}) + D(1 + E_{123}) + FE_{1234}$$

$$r_2 = AE_{234(23)(24)(34)} + BE_{134(13)(14)(34)} + CE_{124(12)(14)(24)} + DE_{123(12)(13)(23)} + FE_{(12)(13)(14)(23)(24)(34)}$$

$$r_3 = AE_{(23)(24)(34)(234)} + BE_{(13)(14)(34)(134)} + CE_{(12)(14)(24)(124)} + DE_{(12)(13)(23)(123)} + FE_{(123)(124)(134)(234)}$$

$$r_4 = AE_{(234)} + BE_{(134)} + CE_{(124)} + DE_{(123)} + FE_{(1234)}$$

$$l_1 = E_{1234}, l_2 = E_{(12)(13)(14)(23)(24)(34)}, l_3 = E_{(123)(124)(134)(234)}, l_4 = E_{(1234)}$$

5) Divide the resulting number by $\hat{\sigma}$ to get the updated turbulent velocity.

6) If the desired number of turbulence values have been generated, stop. Otherwise, go to step 2. The coefficients, A , B , etc., are calculated each time in the loop (steps 2-6) because, in general, σ , L , and V vary with time.

Conclusions

Extremely good rational approximations to the von Kármán longitudinal and transverse spectra were presented. These

spectra were used to develop explicit difference equations suitable for Monte Carlo simulation of turbulence. Calculated spectra of the simulated turbulence show excellent agreement with von Kármán spectra. The resulting method combines the computational simplicity of rational spectra with the accuracy of the irrational von Kármán spectra. The turbulence generated is one dimensional, i.e., varies only along the flight path. The von Kármán approximant approach can be used to generate turbulent gusts, gust gradients, or several simulated turbulence time histories with realistic cross correlation. The addition of three-dimensional realism by the latter method is currently under study.

Acknowledgment

The author is grateful to W. Frost and K.H. Wang of the University of Tennessee Space Institute for their guidance concerning transients in the difference equations.

References

- Wang, S.T. and Frost, W., "Atmospheric Turbulence Simulation Techniques With Application to Flight Analysis," NASA CR 3309, Contract NAS8-32692, Sept. 1980.
- Tatom, F.B. and Smith, S.R., "Atmospheric Turbulence Simulation for Shuttle Orbiter," Summary Report, NASA Contract NAS8-33076, Aug. 1979.
- Van Dyke, M., "Computer-Extended Series," *Annual Review of Fluid Mechanics*, Vol. 16, 1984, pp. 287-309.
- Khovanskii, A.N., *The Application of Continued Fractions and Their Generalizations to Problems in Approximation Theory*, P. Noordhoff, Ltd., Groningen, The Netherlands, 1963.
- Neuman, F. and Foster, J.D., "Investigation of a Digital Automatic Aircraft Landing System in Turbulence," NASA TN D-6066, Oct. 1970.